

## ANALYSIS OF THE 50 KG TOROIDAL FIELD COIL FOR HIGH FIELD ORMAK\*

W. F. Gauster and P. L. Walstrom

Oak Ridge National Laboratory  
Oak Ridge, Tennessee 37830

## NOTICE

This report was prepared as an account of work sponsored by the United States Government. Neither the United States nor the United States Atomic Energy Commission, nor any of their employees, nor any of their contractors, subcontractors, or their employees, makes any warranty, express or implied, or assumes any legal liability or responsibility for the accuracy, completeness or usefulness of any information, apparatus, product or process disclosed, or represents that its use would not infringe privately owned rights.

SUMMARY

Due to space limitations on the windings, the power efficiencies of toroidal field coils for tokamak experiments are in general rather poor. Very substantial improvement can be achieved by using asymmetrical magnet coil designs. The results of mathematical analysis and electric current flow plotting <sup>for</sup> of various types of asymmetrical coil designs are discussed, and numerical data of resistance measurements with the High Field ORMAK prototype coil are given.

I. INTRODUCTION

When non-superconducting toroidal magnet systems are used for tokamak experiments, it is obviously important to design windings with minimum resistance and, therefore, reduced power demand. One possibility is to employ, instead of coils with the usual rectangular cross section (Fig. 1A), wedge-shaped coils (Fig. 1B) which provide larger winding cross section. A detailed discussion of torus windings with wedge-shaped coils has been presented by B. Oswald.<sup>1</sup> A disadvantage of such windings is the poor

\* Research sponsored by the U.S. Atomic Energy Commission under contract with the Union Carbide Corporation.

**MASTER**

accessibility for diagnostics and particle injection. For tokamak experiments, the free space inside the torus windings should be as large as possible in order to provide sufficient flux area for ohmic heating. Therefore, the winding depth next to the torus axis should be as small as possible.

This paper discusses the idea of using asymmetric coil windings, which can be made relatively thin at the inner side of the torus (toward the vertical torus axis) and which reduce the power demand by providing ample thickness toward the outside of the torus. Figure 2A shows an asymmetric torus winding with constant axial width of the coils; Fig. 2B shows one with variable coil width. Obviously, the second design sacrifices accessibility for lower resistance. In the following, we consider only the first type.

Figure 3 (which is self-explanatory) shows various types of asymmetric magnet coils. A prototype coil for the ORNL High Field ORMAK project has been built. The rectangular shape with rounded corners (Fig. 3C) has been chosen, and the detailed design data and technology applied are described in another paper presented at this conference.<sup>2</sup>

Detailed mathematical analysis of and the application of electric current flow plotting to various types of asymmetric magnet coil designs and the results of resistance measurements with the prototype coil are given elsewhere.<sup>3-7</sup> Here, we restrict ourselves to a brief presentation of the most relevant points of these investigations.

## II. ASYMMETRIC COILS WITH EQUAL PARTITION OF RADIAL WIDTH

We consider two types of asymmetric coil windings: coils with equal-partition of radial width and resistance optimized coils. Figure 4A

illustrates the principle of the first, Fig. 4B the principle of the second type. Both coils have six turns. We wrote computer programs for determining the resistance of coils with equipartition of radial width. These were applied to the shapes shown in Figs. 3A and 3B. The calculated resistances were compared with the resistance  $R_0$  of a coil with a symmetric torus winding (Fig. 1A) with  $r_1 = 13.1$  in.;  $r_2 = 14.7$  in.;  $r_3 = 31.6$  in., i.e.,  $\alpha = r_2/r_1 = 1.12$  and  $A = r_3/r_1 = 2.41$ . It should be mentioned that for wedge-shaped coils (Fig. 1B) with these geometrical data, the value of  $R/R_0 = 1.68$ .

We consider first a circular eccentric coil (Fig. 3A) and define  $\alpha_m = (r_1 + a)/r_1$ . For various values of  $\alpha_m$  the resistance ratio  $R/R_0$  is shown in Fig. 5A. For  $\alpha_m = \alpha = 1.12$  we obtain a value  $R/R_0 = 2$  with  $k \approx 5$ . It can be shown that for very small  $\alpha_m$  (i.e.,  $a \ll r_1$ ) the ratio  $R/R_0$  approaches the value  $\sqrt{k}$ . With larger values of  $\alpha_m$ , larger values of  $k$  are necessary for reaching specified values of  $R_0/R$ .

Figure 5B shows  $R_0/R$  vs  $k$  for circular concentric coils with one flat end (see Fig. 3B with  $k' = k$ ). In comparison to Fig. 5A, the ratio  $R_0/R$  increases much faster with increasing values of  $k$ .  $R/R_0 = 2$  is achieved with  $k \approx 2.5$ . It can be shown that for  $a \ll r_1$ , the value  $R_0/R$  is proportional to  $k$ . It is of interest that for any  $\alpha_m > 1.0$ , the value of  $R_0/R$  reaches a maximum for a certain  $k$ . This is clearly shown by the curve  $\alpha_m = 1.4$  in Fig. 5B. More details (e.g., calculation of the resistance ratio for circular concentric coils with two flat ends as shown in Fig. 3B) are presented in Ref. 4.

### III. RESISTANCE OPTIMIZED ASYMMETRIC COILS

The six turns of the resistance optimized coil shown schematically in Fig. 4B have different cross sections. The contour lines of the turns were determined by means of electric current flow plotting.<sup>5</sup> An "analog field plotter" was used. In essence, it consists of a power unit, a voltage divider, and a null detector. Boundaries with constant potential  $V$  were represented by electrodes painted on a conducting paper ("current plotting paper") with a special silver paint. The resistance per square of the silver paint is about  $10^3$  smaller than that of the paper. Using a so-called "tracing stylus," the potential of any point on the current plotting paper can be determined, and by moving from point to point with one specified value of the potential  $V$ , equipotential lines can be traced. It can be shown<sup>6</sup> that by dividing the potential into  $n$  equal parts and tracing the corresponding  $(n-1)$  equipotential lines between the electrodes, the contour lines of turns with equal current can be obtained. In Fig. 4B, the equipotential line  $V = 0$  corresponds to the outer rim and the  $V = 100$  equipotential line to the inner bore of the coil. The potential lines representing the contours of the six turns correspond to potential values which are integral multiples of  $100/6$ . The resistance of such a coil is a minimum and the resistance of all turns are equal.

It is possible to design a coil (similar to the Bitter coils) using circular eccentric plates (Fig. 3A). Due to the "free flow" of the electric current, the resistance is a minimum. This resistance and the current density distribution can be calculated analytically.<sup>4</sup>

#### IV. RESISTANCE MEASUREMENTS WITH THE ORMAK PROTOTYPE COIL<sup>7</sup>

The relative values of the resistances of the six turns for the coil with equal partition of radial width, as shown in Fig. 4A, were measured with the conducting paper field plotter, and the result was  $R_I : R_{II} : \dots : R_{VI} = 21.8 : 19.4 : 17.9 : 15.7 : 13.6 : 11.6$ . A similar measurement with the resistance optimized coil (Fig. 4B) yielded (with an accuracy better than  $\pm 1\%$ ) equal values.

The resistance  $R_0$  of a six turn circular concentric coil with winding thickness  $a$  (Fig. 6, broken line) can be easily calculated. The ratio of the resistances  $R_1$  of the coil with equal partition of radial width (Fig. 4A) to  $R_0$  was measured with the analog field plotter. It was found to be  $R_0/R_1 = 1.96$ . Similarly, the ratio of the resistance  $R_0$  to  $R_2$ , the resistance of the optimized coil, was measured to be  $R_0/R_2 = 2.20$ . This means that the ratio of the resistance  $R_1$  of the coil with equal partition of radial width (Fig. 4A) to the resistance  $R_2$  of the resistance-optimized coil (Fig. 4B) is  $2.20 : 1.96 = 1.12$ .

The actual design of the six-turn prototype coil provides a groove of 0.405 in. width on the inside of each turn for the accommodation of the "cooling conductor," a 3/8 in. square hollow copper conductor with a 0.265 in. diameter circular hole (for the liquid nitrogen cooling), plus space for the insulation between the turns. The contour lines of the turns were determined with a conducting paper field plot for a homogeneous resistance-optimized coil (i.e., without any groove) and then the paper strip corresponding to the groove was cut away. Finally, connections

between the turns were added. Two sheets of metal were machined in the shape of the described paper model (one of copper and one of aluminum 6061/T6), and resistance measurements at room temperature were made with the aluminum coil (the copper coil was used for other purposes). After converting the resistance values from aluminum to copper of the same geometry, the influence of the parallel cooling conductor was considered by calculation. We will designate the resistance found in this way by  $R_2^*$ . Finally, the resistance  $R_0^*$  of a concentric circular copper coil (Fig. 6, broken line) with the same cooling conductor was calculated. The ratio  $R_0^*/R_2^*$  was found to be 2.10, i.e., 4.5% smaller than the resistance ratio  $R_0/R_2 = 2.20$  of similar coils without cooling conductor. Of course, it would be possible to find the actual optimum contours of the turns considering the cooling conductor and crossovers; however, the gain to be expected is so small that this additional work was not done.

Finally, we would like to make the following remark: Further calculations for the design of an ORMAK torus winding with asymmetric coils showed that it would be sufficient (and desirable for mechanical reasons) to provide a cooling conductor with a smaller hole diameter. The temperature rise of the winding parts closest to the torus axis for such an asymmetric design is required to be no larger than that of a concentric design. Under these conditions, the resistance of the asymmetric coil would be further reduced. This results from an increase of the copper volume and from a more favorable temperature distribution during the current pulse.

We acknowledge the valuable contributions of W. J. Schill in producing excellent current flow plots.

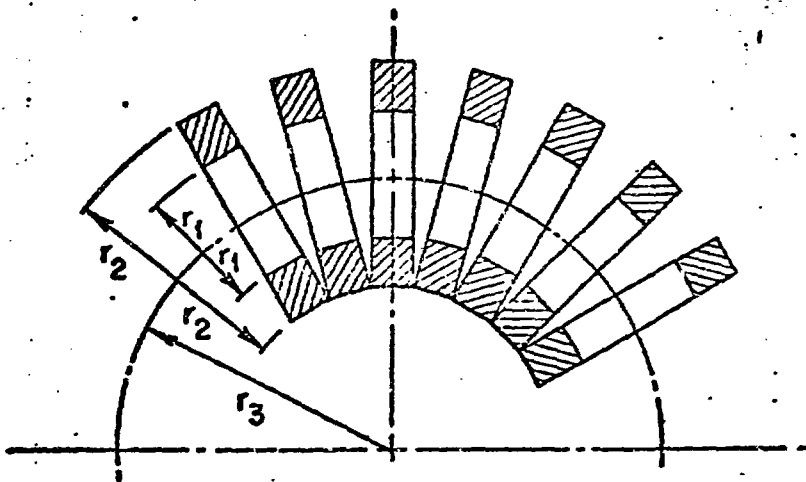
REFERENCES

1. B. Oswald, "Berechnungsgrundlage, Optimierung und Kostfaktoren normalleitender Kryotechnischer und Supraleitender Magnete für die experimentelle Plasmaphysik," Max-Planck Institut für Plasmaphysik Report No. IPP 4/96 (November 1971). See also, D. B. Montgomery, Progress Report, Francis Bitter National Magnet Laboratory, July-December 1971, MIT-NML-PR-71/2, p. 117.
2. J. N. Luton, W. C. T. Stoddart, R. L. Brown, and R. W. Derby, "Development of the 50 kG Toroidal Coil for High Field ORMAK."
3. Thermonuclear Division Annual Progress Report for Period Ending December 31, 1970, ORNL-4688, pp. 44-66.
4. W. F. Gauster and P. L. Walstrom, ORNL-TM-4336 (August 1973).
5. W. F. Gauster and W. J. Schill, ORNL Thermonuclear Division Eng. Sci. Memo No. 119 (June 1973) and No. 124 (July 1973).
6. W. F. Gauster, ORNL Thermonuclear Division Eng. Sci. Memo No. 121 (June 1973).
7. W. F. Gauster and P. L. Walstrom, ORNL Thermonuclear Division Eng. Sci. Memo No. 132 (Sept. 1973).

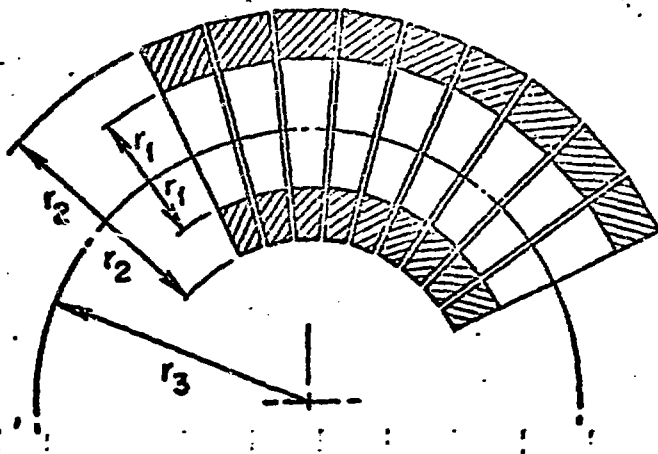
FIGURE CAPTIONS

- Figure 1      Circular Concentric Coil Windings
- A)    Rectangular Cross Section
  - B)    Variable Axial Width
- Figure        Asymmetric Coil Windings
- A)    Rectangular Cross Section
  - B)    Variable Axial Width
- Figure 3      Types of Asymmetric Coils
- Figure 4      Determination of Winding Contours in an Asymmetric Coil
- A)    Radial Width Equally Partitioned
  - B)    Resistance Optimized
- Figure 5      Resistance Ratios of Asymmetric Coils (Equipartition of Radial Width)
- A)    Circular Eccentric
  - B)    Circular with Flat End
- Figure 6      Resistance of ORMAK Prototype Coil





(a)



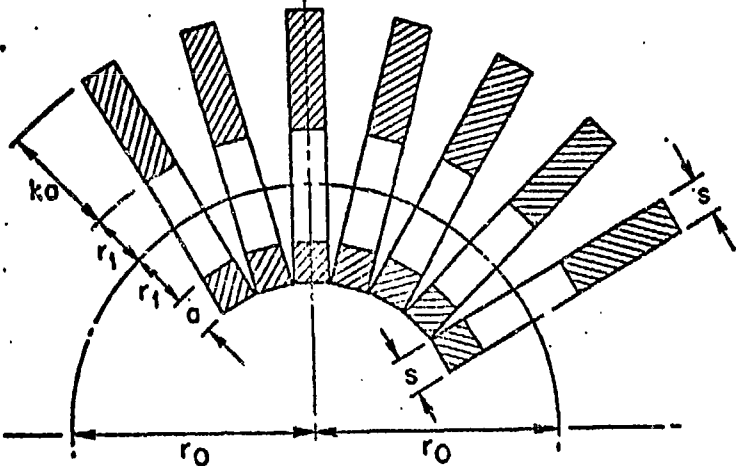
(b)

Figure 1.

W. O. # 91556  
ONR DNG. 73-10666

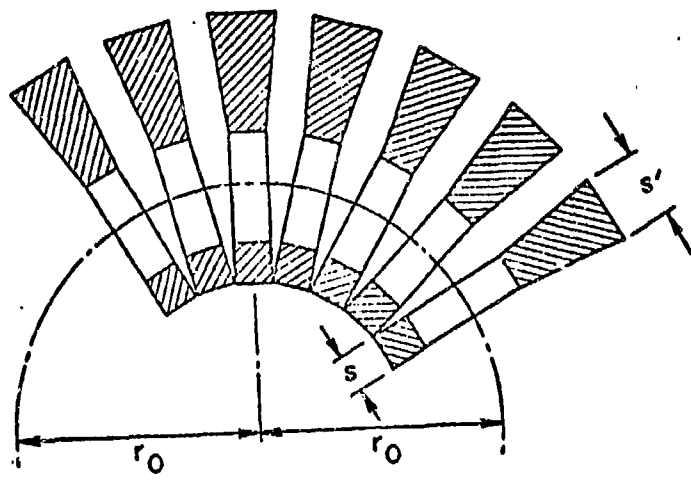
TORI WITH ASYMMETRIC COILS  
(PLAN VIEW)

}  
on slide only (2)



CONSTANT AXIAL WIDTH

(a.)



$s' > s$

VARIABLE AXIAL WIDTH

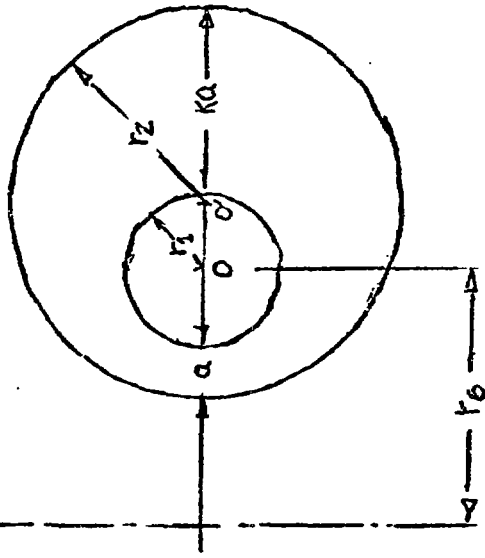
(b.)

Figure 2

# Types of Asymmetrical Coils

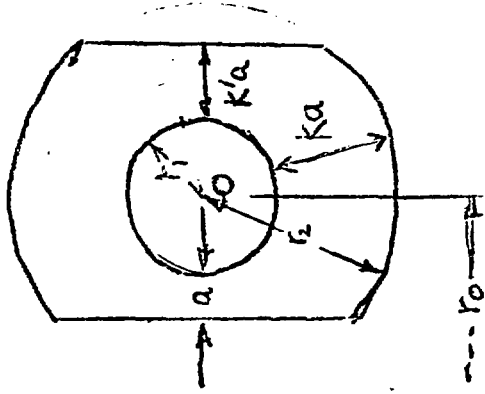
$$\alpha_m = \frac{r_1 + a}{r_1}; \quad \alpha_M = \frac{r_1 + ka}{r_1}$$

TORUS  
AXIS



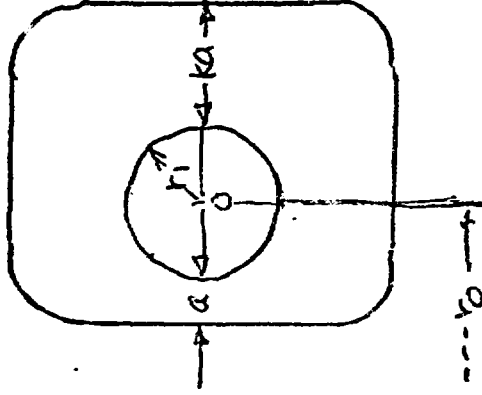
CIRCULAR ECCENTRIC

(a)



CIRCULAR CONCENTRIC  
WITH FLAT ENDS

(b)



RECTANGULAR WITH ROUNDED  
CORNERS

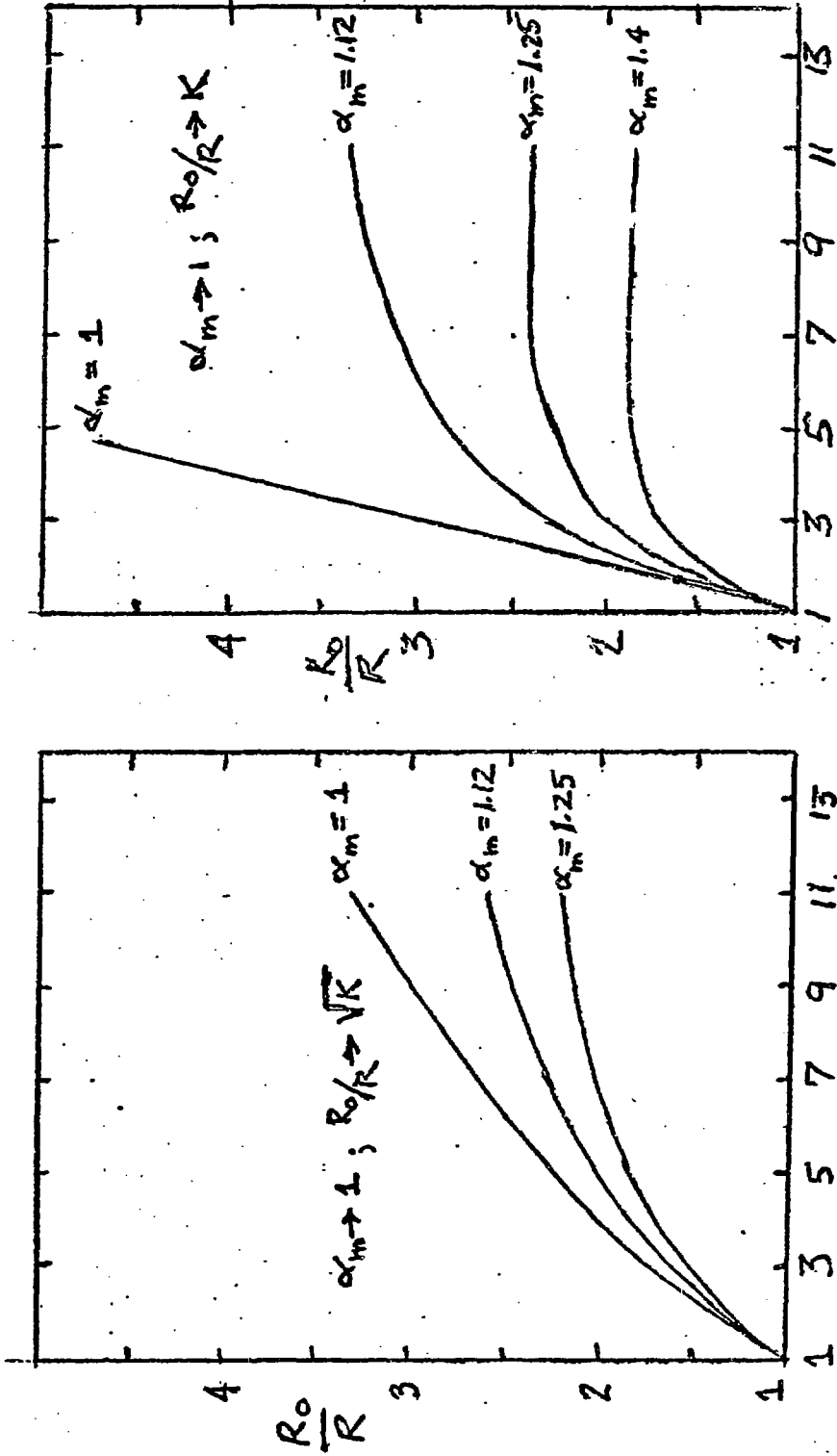
(c)

Figure 3

# Figure 5

## RESISTANCE RATIOS OF ASYMMETRICAL MAGNET COILS

(Equipartition of Radial Width)



CIRCULAR ECCENTRIC

CIRCULAR FLAT END

(a) HOMOGENEOUS

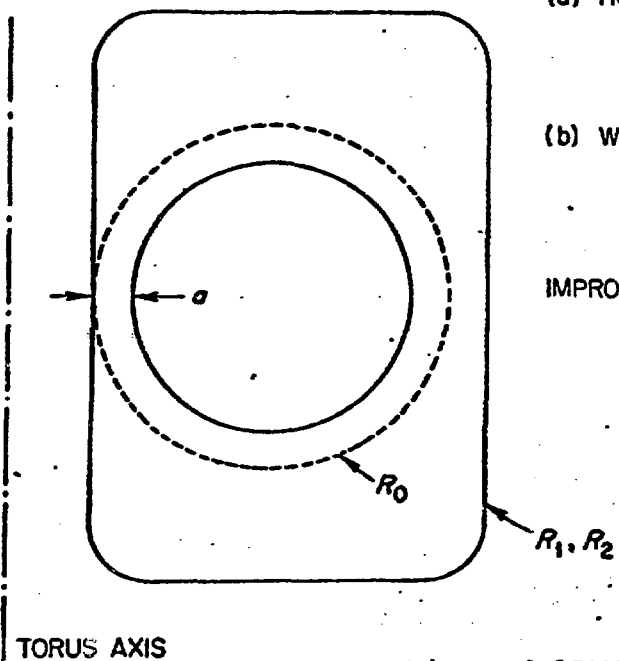
- $R_0$  CONCENTRIC WITH "EQUAL PARTITION"
- $R_1$  ASYMMETRIC WITH "EQUAL PARTITION"
- $R_2$  RESISTANCE OPTIMIZED ASYMMETRIC COIL

(b) WITH COOLING CHANNEL  $R_0^*$ ;  $R_1^*$ ;  $R_2^*$

$$\frac{R_0}{R_1} = 1.96 ; \frac{R_0}{R_2} = 2.20 ; \frac{R_0^*}{R_2^*} = 2.10$$

IMPROVEMENTS DUE TO MORE ADVANCED DESIGN

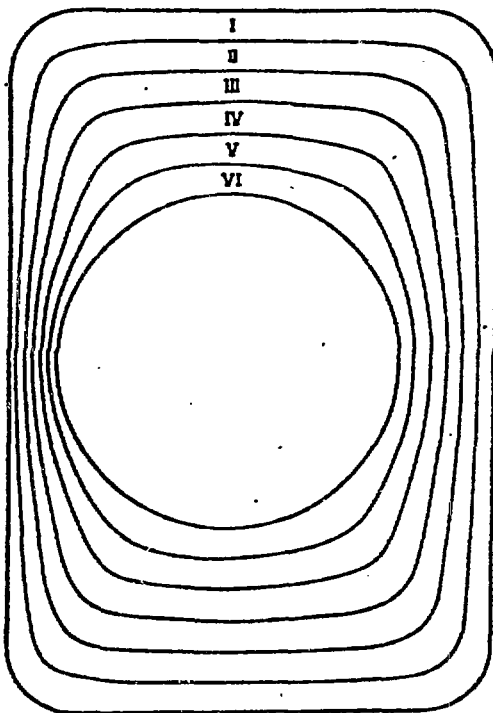
- (a) SMALLER COOLING CHANNELS
- (b) NONUNIFORM TEMPERATURE DISTRIBUTION DURING CURRENT PULSE



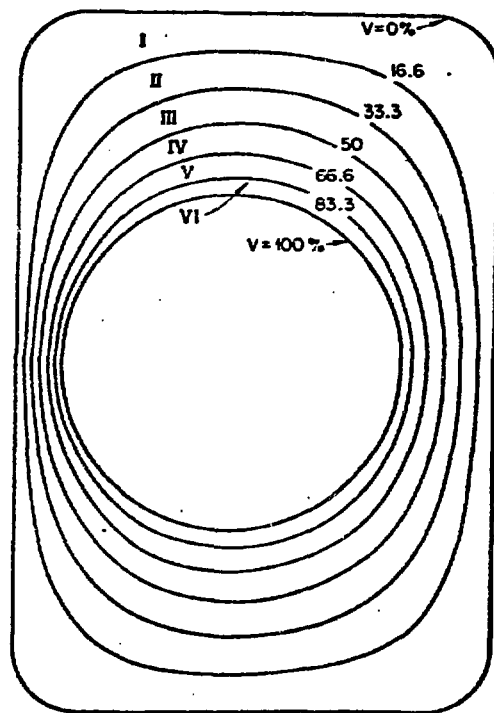
Resistance of ORMAK Prototype Coil.  
(W.F. Gauster and P.L. Walstrom, Eng. Sc. Memo No. 132)

*Figure 6*

Different Types of Asymmetrical Coils.



COIL WITH EQUIPARTITION OF RADIAL WIDTH  
W.F. GAUSTER AND P.L. WALSTROM, ORNL-TM-4336



RESISTANCE OPTIMIZED COIL  
W.F. GAUSTER, ENG. SC. MEMO NO. 121

*Figure 8*